Clearly, III is not favored by either steric factors or RO-to-M π bonding. The difference in geometry may result from the fact that the M≡M bond, which is weaker than M≡N, M≡C, and M—NO bonds in these compounds, is more sensitive to bond weakening by axial ligand coordination. The structures of $W_2Me_2(O_2CNEt_2)_4$ and $W_2(O_2CNMe_2)_6$ show that axial coordination is avoided relative to coordination in the *xy* plane.[6]

Detailed studies of the electronic structures of these fascinating molecules are planned.

Experimental Section

The compounds $(t\text{-BuO})_3W{\equiv}CMe$ and $(t\text{-BuO})_3W{\equiv}N$ were prepared from the reactions between $W_2(O\text{-}t\text{-Bu})_6$ and MeC≡CMe and MeC≡N as described by Schrock.[5]

The alkylidyne complex was purified by vacuum sublimation (40 °C, 10^{-4} torr). Because it is extremely soluble in hydrocarbon solvents, crystallization from solution was not successful. Crystals suitable for X-ray studies were obtained by sublimation.

The nitrido compound was purified by sublimation (110 °C, 10^{-4} torr) and crystallized from hot toluene. (It is only very sparingly soluble in hydrocarbon solvents at room temperature.) Long hexagonal rods were obtained in this manner.

X-ray Crystallography. General procedures and a library of programs have been given previously.[14]

$[(t\text{-BuO})_3W{\equiv}CMe]_2$. Colorless crystals were transferred to a nitrogen-filled glovebag in sealed ampules. The sample appeared highly reactive, darkening immediately when the ampules were opened, although subsequent examination indicated crystals of excellent quality. A systematic search of a limited hemisphere of reciprocal space revealed no systematic absences or symmetry, leading to the assignment of the triclinic space group. Complete crystallographic data are given in Table V. The structure was solved by Patterson and Fourier techniques. ψ scans of several reflections indicated a maximum variation of 5% in ψ, so no absorption correction was applied. All hydrogen atoms were located, and the final full-matrix refinement included all postional parameters, isotropic thermal parameters for hydrogen atoms, and anisotropic thermal parameters for non-hydrogen atoms. A final difference Fourier was featureless, the largest peak (1.3 e/Å^3) lying 0.4 Å from the tungsten.

$[(t\text{-BuO})_3W{\equiv}N]_x$. A hexagonal needle approximately 0.05 mm in diameter was cleaved to yield a well-formed prism 0.24 mm in length. A systematic search of limited hemispheres of reciprocal space revealed a trigonal lattice with a general pseudoextinction such that all *hkl* for $l = 2n + 1$ were weak. It was difficult to determine what, if any, space group extinctions were present because of the psuedoextinction. Crystal and diffractometer data are given in Table V.

The structure was initially solved in space group $P3c1$ by placing the tungsten atom at $z = {}^1/_4$ on the *c* axis. A difference Fourier phased on the tungsten ($R(F) = 0.14$) revealed all remaining non-hydrogen atoms. Full-matrix refinement converged to $R(F) = 0.028$. Examination of the coordinates at this stage revealed that all atoms were within 1 σ of a higher order symmetry, and the space group was thus transformed to $P6_3cm$. Full-matrix refinement in this setting rapidly converged to $R(F) = 0.017$, indicating the proper setting. A final difference Fourier was featureless, the largest peak being 0.6 e/Å^3.

Acknowledgment. We thank the National Science Foundation and the Wrubel Computing Center for support.

Registry No. $(t\text{-BuO})_3W{\equiv}CMe$, 86669-24-1; $(t\text{-BuO})_3W{\equiv}N$, 86669-26-3.

Supplementary Material Available: Tables of anisotropic thermal parameters, fractional coordinates, and thermal parameters for hydrogen atoms, complete tables of distances and angles, and listings of observed and calculated structure amplitudes for $[(t\text{-BuO})_3W{\equiv}CMe]_2$ and $[(t\text{-BuO})_3W{\equiv}N]_x$ (24 pages). Ordering information is given on any current masthead page. Crystallographic data are also available, in microfiche form, from the Chemistry Library, Indiana University Chemistry Department. Request MSC Report No. 82083 for $[(t\text{-BuO})_3W{\equiv}CMe]_2$ and 82087 for $[(t\text{-BuO})_3W{\equiv}N]_x$.

---

(14) Huffman, J. C.; Lewis, L. N.; Caulton, K. G. *Inorg. Chem.* **1980**, *19*, 2755.

Contribution from the Department of Chemistry, Purdue University, West Lafayette, Indiana 47907,
and the Molecular Structure Center, Indiana University, Bloomington, Indiana 47405

Dinuclear Aryloxide Chemistry. 1. A Direct Comparison of Aryloxide and Alkoxide Coordination to a Dimetal Center. Synthesis and Structure of 1,2-Bis(isopropoxy)tetrakis(2,6-dimethylphenoxy)dimolybdenum (Mo≡Mo)

TIMOTHY W. COFFINDAFFER,[†] IAN P. ROTHWELL,*[†] and JOHN C. HUFFMAN[‡]

Received January 11, 1983

The preparation and characterization of the compound $1,2\text{-}Mo_2(O\text{-}i\text{-}Pr)_2(OAr)_4$ (OAr = 2,6-dimethylphenoxide) are reported. Structural analysis of the compound has allowed a direct comparison of alkoxide and aryloxide coordination to a dimetal center from which it was concluded that although not expected to be as good a π-donor ligand as alkoxide, aryloxide has a greater ability to form large M–O–C angles and thus relieve steric strain at the metal. Crystal data for $Mo_2(O\text{-}i\text{-}Pr)_2(OAr)_4$ at −163 °C were $a = 18.169$ (6) Å, $b = 11.327$ (3) Å, $c = 10.678$ (3) Å, $\alpha = 99.58$ (2)°, $\beta = 57.82$ (2)°, $\gamma = 97.63$ (2)°, $Z = 2$, and $d_{\text{calcd}} = 1.441$ g cm^{-3}, with space group $P\bar{1}$.

Introduction

One important characteristic of early-transition-metal alkoxide chemistry is the ability of the ligand to undergo oxygen p-to-metal-d π bonding.[1] This has been used to account for a number of physical and chemical properties of alkoxides. Structural studies have shown that M–O distances associated with alkoxy groups can be very short, implying varying amounts of multiple bond character. Similarly π donation by the alkoxy group is associated with large M–O–C angles, sometimes 160°, and this is rationalized as being due to partial rehybridization at the oxygen to promote the nonbonding lone pairs into p orbitals of correct symmetry for overlap with metal d orbitals. In the extreme case, a linear M–O–C unit con-

---

[†] Purdue University.
[‡] Indiana University.

(1) (a) For a review of metal alkoxide chemistry see: Bradley, D. C.; Mehrotra, R. C.; Gaur, D. P. "Metal Alkoxides"; Academic Press: London, New York, San Francisco, 1978. (b) A review of metal phenoxides has recently been published; see: Malhotra, K. C.; Martin, R. L. *J. Organomet. Chem.* **1982**, *239*, 159.

0020-1669/83/1322-2906$01.50/0

Table I. Fractional Coordinates and Isotropic Thermal Parameters for $Mo_2(O\text{-}i\text{-}Pr)_2(OC_8H_9)_4$

atom	10^4x	10^4y	10^4z	$10B_{iso}$, $Å^2$
Mo(1)	5535.6 (3)	4624.4 (5)	10021 (1)	16
O(2)	4813 (3)	3596 (4)	11488 (5)	32
C(3)	5080 (5)	2877 (11)	12163 (14)	94
C(4)	4575 (8)	1911 (11)	12643 (18)	113
C(5)	6013 (5)	3000 (7)	11616 (8)	36
O(6)	6094 (3)	5943 (4)	10611 (5)	22
C(7)	6044 (4)	7116 (6)	11210 (7)	23
C(8)	5602 (4)	7372 (6)	12776 (7)	24
C(9)	5606 (4)	8557 (7)	13367 (8)	31
C(10)	6037 (5)	9465 (7)	12450 (9)	33
C(11)	6477 (4)	9191 (7)	10939 (8)	31
C(12)	6496 (4)	8026 (6)	10277 (7)	26
C(13)	5177 (4)	6358 (7)	13724 (8)	29
C(14)	7019 (5)	7701 (7)	8624 (8)	33
O(15)	6303 (2)	3856 (4)	8097 (4)	20
C(16)	6547 (4)	3330 (6)	6684 (6)	20
C(17)	6955 (4)	4034 (6)	5509 (7)	23
C(18)	7220 (4)	3478 (7)	4079 (7)	28
C(19)	7086 (4)	2255 (8)	3851 (8)	35
C(20)	6691 (4)	1564 (6)	5026 (8)	28
C(21)	6406 (4)	2083 (6)	6487 (7)	24
C(22)	7108 (5)	5358 (6)	5801 (8)	32
C(23)	5973 (5)	1364 (6)	7767 (8)	29
Mo(1A)	9427.8 (3)	4602.7 (4)	10983 (1)	11
O(2A)	10069 (2)	3815 (3)	11491 (4)	15
C(3A)	9632 (4)	3074 (5)	12718 (7)	16
C(4A)	9406 (4)	3838 (6)	14154 (7)	26
C(5A)	10250 (5)	2127 (6)	12339 (8)	26
O(6A)	8764 (2)	3594 (3)	10287 (4)	16
C(7A)	8618 (4)	2799 (5)	9323 (6)	16
C(8A)	8794 (4)	1595 (5)	9144 (6)	17
C(9A)	8579 (4)	781 (5)	8250 (7)	22
C(10A)	8218 (4)	1134 (6)	7520 (7)	22
C(11A)	8060 (4)	2335 (6)	7696 (7)	18
C(12A)	8264 (4)	3180 (5)	8587 (6)	17
C(13A)	9187 (4)	1224 (5)	9947 (7)	22
C(14A)	8105 (4)	4486 (6)	8747 (8)	23
O(15A)	8828 (2)	5912 (3)	12400 (4)	17
C(16A)	8747 (4)	7128 (5)	12731 (6)	16
C(17A)	9069 (4)	7765 (5)	13596 (6)	17
C(18A)	8952 (4)	8983 (6)	13966 (7)	24
C(19A)	8495 (5)	9549 (6)	13563 (8)	29
C(20A)	8164 (4)	8900 (6)	12742 (8)	25
C(21A)	8272 (4)	7677 (5)	12321 (6)	19
C(22A)	9516 (4)	7144 (5)	14148 (7)	19
C(23A)	7912 (4)	6952 (6)	11446 (8)	25

Table II. Bond Distances (Å) for $Mo_2(O\text{-}i\text{-}Pr)_2(OC_6H_9)_4$

molecule 1			molecule 2		
Mo(1)	Mo(1)	2.249 (1)	Mo(1A)	Mo(1A)	2.241 (1)
Mo(1)	O(2)	1.883 (4)	Mo(1A)	O(2A)	1.886 (4)
Mo(1)	O(6)	1.904 (4)	Mo(1A)	O(6A)	1.902 (4)
Mo(1)	O(15)	1.896 (4)	Mo(1A)	O(15A)	1.898 (4)
O(2)	C(3)	1.446 (8)	O(2A)	C(3A)	1.460 (7)
O(6)	C(7)	1.367 (7)	O(6A)	C(7A)	1.364 (7)
O(15)	C(16)	1.374 (7)	O(15A)	C(16A)	1.371 (7)
C(3)	C(4)	1.313 (13)	C(3A)	C(4A)	1.501 (9)
C(3)	C(5)	1.463 (11)	C(3A)	C(5A)	1.506 (9)
C(7)	C(8)	1.412 (9)	C(7A)	C(8A)	1.400 (8)
C(7)	C(12)	1.405 (9)	C(7A)	C(12A)	1.395 (8)
C(8)	C(9)	1.385 (9)	C(8A)	C(9A)	1.387 (9)
C(8)	C(13)	1.503 (10)	C(8A)	C(13A)	1.508 (9)
C(9)	C(10)	1.390 (11)	C(9A)	C(10A)	1.384 (9)
C(10)	C(11)	1.365 (10)	C(10A)	C(11A)	1.390 (9)
C(11)	C(12)	1.384 (10)	C(11A)	C(12A)	1.391 (8)
C(12)	C(14)	1.498 (10)	C(12A)	C(14A)	1.509 (9)
C(16)	C(17)	1.394 (9)	C(16A)	C(17A)	1.399 (8)
C(16)	C(21)	1.403 (9)	C(16A)	C(21A)	1.398 (8)
C(17)	C(18)	1.392 (9)	C(17A)	C(18A)	1.383 (9)
C(17)	C(22)	1.500 (10)	C(17A)	C(22A)	1.517 (8)
C(18)	C(19)	1.377 (10)	C(18A)	C(19A)	1.378 (9)
C(19)	C(20)	1.386 (11)	C(19A)	C(20A)	1.379 (10)
C(20)	C(21)	1.401 (9)	C(20A)	C(21A)	1.389 (9)
C(21)	C(23)	1.485 (10)	C(21A)	C(23A)	1.493 (9)

taining sp-hybridized oxygen would in theory allow the π donation of four-electrons to the metal, which could be represented $\mathrm{M}\overset{\leftarrow}{\underset{\leftarrow}{\text{—}}}\mathrm{O}\text{—}\mathrm{C}$. However, such a situation is rare as suitable orbitals at the metal are normally lacking. It must also be remembered that a steric contribution is sometimes made to this angle increase. The strength of early-transition-metal–alkoxide bonds[2] can be attributed to this phenomenon, as can the fact that as one decreases the electron deficiency of the metal (i.e., moves to the right across the d block) then the number and stability of metal alkoxides decrease.[1] Chemically, recent interest in alkoxy ligands has arisen through the realization (both theoretical[3] and practical[4]) that such π-donor ligands can have a favorable effect on important organometallic reactions such as transition-metal-catalyzed olefin metathesis. Also the presence of π-donating alkoxide groups in a molecule can greatly increase the amount of π back-bonding from a metal to suitable π-acid ligands such as CO[5] and bpy,[6] with dramatic chemical and structural consequences.

Our group is at present carrying out a systematic study of the chemistry of early-transition-metal aryloxides, and in particular 2,6-dialkylphenoxides. A number of structures of such compounds have been carried out,[7] and we have noticed that these ligands consistently coordinate with large M–O–Ar angles. For example, in $Zr(OAr')_2(CH_2C_6H_5)_2$ (OAr′ = 2,6-di-*tert*-butylphenoxide) the Zr–O–Ar′ angles are almost linear.[8] A component of this opening up to the angle is clearly steric, although the molecule can accommodate a considerable amount of bending at the oxygen atom with no apparent increase of nonbonding interactions with the metal or other ligands. As the number of structures of early-transition-metal aryloxides is relatively small compared to those of alkoxides, we decided to synthesize and structurally study a compound that contained both alkoxide and aryloxide ligands coordinated to the same metal center. This allows a direct comparison of the two types of ligand, and our results are outlined in this paper.

Results and Discussion

Synthesis. Addition of 2,6-dimethylphenol (excess) to hydrocarbon solutions of $Mo_2(O\text{-}i\text{-}Pr)_6$ (M≡M) at 25 °C leads to the initial formation of 1,2-$Mo_2(O\text{-}i\text{-}Pr)_2(OAr)_4$ (I) (OAr = 2,6-dimethylphenoxide) and elimination of 4 equiv of isopropyl alcohol. Removal of solvent and generated isopropyl alcohol followed by redissolving in hexane and cooling allowed red-orange crystals of the product to be isolated. If the solvent is removed from the crude product and a melt formed between

---

(2) Navrotsky, A. In "M.T.P. International Reviews of Science", Series Two; Sharp, D. W. A.; Ed.; University Park Press: Baltimore, 1975; Vol. 5, Chapter 2.

(3) Rappé, A. K.; Goddard, W. A., III. *J. Am. Chem. Soc.* **1982**, *104*, 448.

(4) Schrock, R. R. In "Proceedings of Inorganic Chemistry Towards the 21st Century"; American Chemical Society: Washington, DC, 1982; ACS Symp. Ser.

(5) Chisholm, M. H.; Huffman, J. C.; Kelly, R. L. *J. Am. Chem. Soc.* **1979**, *101*, 7615.

(6) Chisholm, M. H.; Huffman, J. C.; Kelly, R. L. *J. Am. Chem. Soc.* **1981**, *103*, 4945.

(7) (a) Chamberlain, L.; Keddington, J.; Rothwell, I. P.; Huffman, J. C. *J. Chem. Soc., Chem. Commun*, **1982**, 805. (b) Chamberlain, L.; Keddington, J.; Huffman, J. C.; Rothwell, I. P. *Organometallics* **1982**, *1*, 1538. (c) Chamberlain, L.; Rothwell, I. P.; Huffman, J. C. *J. Am. Chem. Soc.*, in press.

(8) (a) Huffman, J. C., personal communication. (b) Similar, although smaller, angle increases have been seen for the simple terminal phenoxide ligand in compounds such as $[TiCl_2(OPh)_2]_2$ (see ref 14) and $[MoCl_2(OPh)_3]_2$ (see ref 1b).

Table III. Bond Angles (deg) for $Mo_2(O\text{-}i\text{-}Pr)_2(OC_8H_9)_4$

molecule 1				molecule 2			
Mo(1)	Mo(1)	O(2)	96.5 (1)	Mo(1A)	Mo(1A)	O(2A)	96.9 (1)
Mo(1)	Mo(1)	O(6)	106.5 (1)	Mo(1A)	Mo(1A)	O(6A)	107.5 (1)
Mo(1)	Mo(1)	O(15)	108.7 (1)	Mo(1A)	Mo(1A)	O(15A)	106.4 (1)
O(2)	Mo(1)	O(6)	115.3 (2)	O(2A)	Mo(1A)	O(6A)	116.0 (2)
O(2)	Mo(1)	O(15)	115.6 (2)	O(2A)	Mo(1A)	O(15A)	113.3 (2)
O(6)	Mo(1)	O(15)	112.5 (2)	O(6A)	Mo(1A)	O(15A)	114.6 (2)
Mo(1)	O(2)	C(3)	126.6 (4)	Mo(1A)	O(2A)	C(3A)	121.1 (3)
Mo(1)	O(6)	C(7)	145.8 (4)	Mo(1A)	O(6A)	C(7A)	157.1 (3)
Mo(1)	O(15)	C(16)	155.4 (4)	Mo(1A)	O(15A)	C(16A)	148.1 (3)
O(2)	C(3)	C(4)	113.8 (9)	O(2A)	C(3A)	C(4A)	109.9 (5)
O(2)	C(3)	C(5)	114.2 (6)	O(2A)	C(3A)	C(5A)	106.5 (5)
C(4)	C(3)	C(5)	125.4 (9)	C(4A)	C(3A)	C(5A)	112.3 (5)
O(6)	C(7)	C(8)	118.4 (6)	O(6A)	C(7A)	C(8A)	118.8 (5)
O(6)	C(7)	C(12)	120.1 (6)	O(6A)	C(7A)	C(12A)	119.9 (5)
C(8)	C(7)	C(12)	121.2 (6)	C(8A)	C(7A)	C(12A)	121.2 (5)
C(7)	C(8)	C(9)	117.8 (7)	C(7A)	C(8A)	C(9A)	118.1 (6)
C(7)	C(8)	C(13)	119.2 (6)	C(7A)	C(8A)	C(13A)	119.5 (5)
C(9)	C(8)	C(13)	122.9 (6)	C(9A)	C(8A)	C(13A)	122.4 (5)
C(8)	C(9)	C(10)	121.2 (7)	C(8A)	C(9A)	C(10A)	121.8 (6)
C(9)	C(10)	C(11)	119.9 (7)	C(9A)	C(10A)	C(11A)	119.2 (6)
C(10)	C(11)	C(12)	121.8 (7)	C(10A)	C(11A)	C(12A)	120.8 (6)
C(7)	C(12)	C(11)	118.0 (6)	C(7A)	C(12A)	C(11A)	118.8 (5)
C(7)	C(12)	C(14)	119.5 (6)	C(7A)	C(12A)	C(14A)	120.8 (5)
C(11)	C(12)	C(14)	122.4 (7)	C(11A)	C(12A)	C(14A)	120.4 (5)
O(15)	C(16)	C(17)	119.5 (6)	O(15A)	C(16A)	C(17A)	118.8 (5)
O(15)	C(16)	C(21)	117.4 (5)	O(15A)	C(16A)	C(21A)	119.1 (5)
C(17)	C(16)	C(21)	123.0 (6)	C(17A)	C(16A)	C(21A)	121.8 (5)
C(16)	C(17)	C(18)	118.5 (6)	C(16A)	C(17A)	C(18A)	118.0 (5)
C(16)	C(17)	C(22)	119.9 (6)	C(16A)	C(17A)	C(22A)	121.5 (5)
C(18)	C(17)	C(22)	121.5 (6)	C(18A)	C(17A)	C(22A)	120.5 (6)
C(17)	C(18)	C(19)	119.8 (7)	C(17A)	C(18A)	C(19A)	121.4 (6)
C(18)	C(19)	C(20)	121.0 (7)	C(18A)	C(19A)	C(20A)	119.7 (6)
C(19)	C(20)	C(21)	121.3 (7)	C(19A)	C(20A)	C(21A)	121.3 (6)
C(16)	C(21)	C(20)	116.3 (6)	C(16A)	C(21A)	C(20A)	117.7 (5)
C(16)	C(21)	C(23)	121.4 (6)	C(16A)	C(21A)	C(23A)	119.9 (5)
C(20)	C(21)	C(23)	122.4 (6)	C(20A)	C(21A)	C(23A)	122.4 (6)

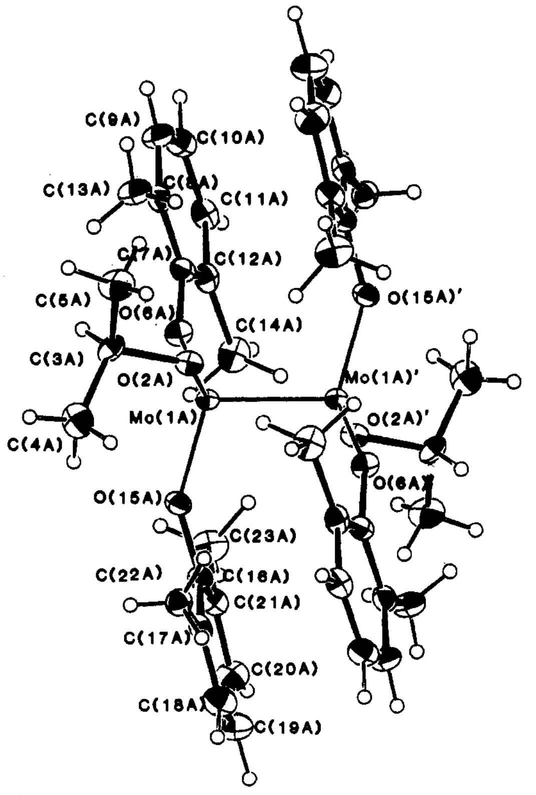

Figure 1. ORTEP view of $Mo_2(O\text{-}i\text{-}Pr)_2(OC_6H_3Me_2)_4$ (molecule 2) showing the atom numbering scheme.

I and ArOH at 100 °C, then 2 more equiv of isopropyl alcohol are eliminated with the formation of the deep-red, sparingly soluble $Mo_2(OAr)_6$ (II).

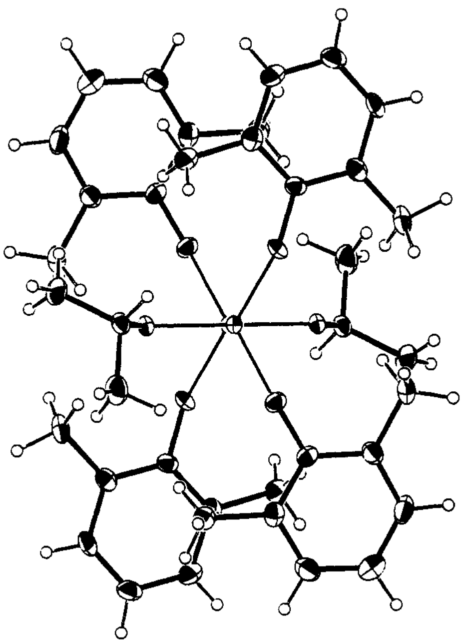

Figure 2. ORTEP view of molecule 2 looking down the Mo≡Mo bond.

Properties. Both I and II are air-sensitive solids, rapidly turning brown and then black on exposure to air. Compound I is appreciably soluble in aromatic hydrocarbon solvents and hexane, whereas II is only sparingly soluble in benzene or toluene at room temperature. ^1H NMR data are given in the Experimental Section.

Solid-State Structure of $Mo_2(O\text{-}i\text{-}Pr)_2(OAr)_4$ (I). Final atomic positional parameters are given in Table I, and bond distances and angles are given in Tables II and III, respectively.

Table IV. Comparison between the Alkoxide and Aryloxide Ligand Bond Distances and Angles

ligand	M–O, Å	O–C, Å	M–O–C, deg	M–M–O, deg
		Molecule 1		
O-*i*-Pr	1.883 (4)	1.446 (8)	126.6 (4)	96.5 (1)
OAr	1.904 (4)	1.367 (7)	145.8 (4)	106.5 (1)
OAr	1.896 (4)	1.374 (7)	155.4 (4)	108.7 (1)
		Molecule 2		
O-*i*-Pr	1.886 (4)	1.460 (7)	121.1 (3)	96.9 (1)
OAr	1.902 (4)	1.364 (7)	157.1 (3)	107.5 (1)
OAr	1.898 (4)	1.371 (7)	148.1 (3)	106.4 (1)

In the solid state, the compound contains two similar but independent molecules (1 and 2), each with a crystallographic inversion center, in the unit cell ($Z = 2$). An ORTEP view of molecule 2 is given in Figure 1 along with the atom numbering scheme, and a view down the Mo–Mo axis is shown in Figure 2. It is noted that the isopropoxy group on molecule 1 appears to have a large vibrational component, even at low temperature. There does not appear, however, to be disorder, as the hydrogen atoms were located and refined.

The Mo-to-Mo distances of 2.249 (1) Å (molecule 1) and 2.241 (1) Å (molecule 2) are in fact the longest so far reported for an unbridged molybdenum–molybdenum triple bond in compounds of the type $\mathrm{Mo_2X_6}$ or $\mathrm{Mo_2X_4Y_2}$,[9] although the difference between this value and that found in $\mathrm{Mo_2(OCH_2CMe_3)_6}$ (2.222 (2) Å)[11] is not particularly significant. Each molybdenum is coordinated to three oxygen atoms with a staggered, ethane-like geometry about the dimetal center. The major difference between molecules 1 and 2 is in the conformation of the $\mathrm{CHMe_2}$ group of the isopropoxide ligands. In molecule 1 the methyl groups are arranged so that they lie roughly parallel with the Mo–Mo axis, whereas in molecule 2 they are twisted to lie almost perpendicular. This has little effect on the coordination geometry about the metal, although it affects slightly the packing of the other groups.

In both molecules the aryl groups of the OAr ligands are approximately coplanar and oriented perpendicular to the Mo–Mo axis. At first sight this is unexpected as it maximizes the steric interactions between the methyl groups on adjacent aryloxy ligands. However, models show that attempts to relieve any steric congestion at each end of the molecule by rotating the aryl planes to lie parallel with the Mo–Mo axis results in considerable amounts of steric interaction between the methyl groups that are brought over the metal–metal bond, with the ligands attached to the second metal. Clearly, the interactions between adjacent aryloxides is thus less in the structure that is adopted rather than the methyl groups lying *proximal* and *distal* to the metal–metal bond, although a compromise with the aryl planes lying at an intermediate angle seems the least overall sterically congested structure.

The most important structural comparison is between the alkoxide and aryloxide ligand bond distances and angles to the metal. These are grouped together in Table IV. A typical bonding description for an $\mathrm{M_2X_6}$ (M = Mo, W) molecule involves the use of the d_{xz} and d_{yz} atomic orbitals (defining the M–M axis as the z axis) for use in forming the Mo–Mo π bonds while one set of the in-plane atomic orbitals (p_x, p_y or $d_{x^2-y^2}$, d_{xy}) is availabile for ligand π bonding.[10] Thus, the three ligands are competing for these two orbitals. It can be seen from Table IV that the Mo-O-*i*-Pr bond is slightly shorter (by 0.017 Å (average) in molecule 1 and 0.014 Å (average) in molecule 2), implying that the alkoxide ligand is a slightly better π-donor ligand. The values of the Mo–O distances, between 1.883 (4) and 1.904 (4) Å, are shorter than would be expected for a bond of order 1. Examination of compounds found in the literature shows that in $\mathrm{Mo_2\ (OCH_2CMe_3)_6}$[11] the distances vary between 1.855 (6) and 1.905 (6) Å whereas in the adduct $\mathrm{Mo_2(OCH_2CMe_3)_6(py)_2}$,[12] where the pyridine molecule reduces to one the number of d orbitals available for π donation, the distances are 1.945 Å (average). One can make the estimate that in the absence of π bonding a purely σ-bonding distance would lie between 2.00 and 2.05 Å to an $\mathrm{(Mo_2)^{6+}}$ center. In a compound where there is only one alkoxy group bonded to each metal, $\mathrm{Mo_2(O\text{-}\mathit{t}\text{-}Bu)_2(CH_2SiMe_3)_4}$,[13] the value drops to 1.865 (8) Å so that a considerable amount of double-bond character is present. Another structural consequence of alkoxide or aryloxide π bonding to this dimetal center is that the dihedral angles between M–M–O and M–O–C are less than 10°. This is a common feature found in all other "Chisholm-type" compounds containing alkoxides as it is the preferred conformation to maximize π overlap with the vacant metal orbitals. In the title compound the *i*-Pr groups are away from the $\mathrm{Mo{\equiv}Mo}$ function while the four Ar groups lie toward the metal–metal bond.

By far the most significant difference between the alkoxide and aryloxide ligands in the structure of I is the value of the M–O–C angles. In molecule 1 the M–O–Ar angle is 25° (average) larger than the M–O-*i*-Pr angle, and in molecule 2 this value is 31.5° (average). We believe that a characteristic difference between early-transition-metal aryloxides and alkoxides is that the aryloxide ligand can more readily open up the M–O–C angle, and typically larger values of this angle will be found in structures containing this group. We attribute this greater flexibility of the aryloxide ligand to the fact that the aryl group can also enter into π-bonding with the oxygen atom.[14] This is the normal rationalization of the higher acidities of phenol vs. aliphatic alcohols and results in the O–Ar bond typically being 0.07 Å shorter than the O–R bond. This competition by the aryl group for the electron density on O would be expected to reduce the ability of the oxygen to π-donate to a coordinated metal. Also, it allows the stabilization of a situation involving a linear M–O–Ar function, and this could be represented $\mathrm{M}\overset{\leftarrow}{-}\mathrm{O}\overset{\rightarrow}{-}\mathrm{Ar}$. Maximum overlap in this case requires the phenyl ring to be oriented coplanar with the d orbital on the metal that is being used for π bonding. This is exactly the conformation found in the title compound with the aryl groups perpendicular to the metal–metal bond (z axis) and coplanar with the $d_{x^2-y^2}$ and d_{xy} orbitals.

Although the solid-state structure contains two environments for the $\mathrm{OC_6H_3\mathit{Me}_2}$ groups, in solution the ^{1}H NMR spectrum shows only one signal for these protons, implying that rapid rotation occurs about the M–O–Ar bond. This solution spectrum is also consistent with the presence of the anti rotamer in solution, as the gauche form would lead to nonequivalent OAr groups. However, it seems reasonable that rotation about the $\mathrm{Mo{\equiv}Mo}$ bond will be facile in this compound,[13] and this process would lead to a single set of signals irrespective of the actual anti-gauche populations in solution.

Concluding Remarks. We conclude that although aryloxide ligands are expected to be slightly weaker π-donor ligands than alkoxides, they have a greater ability to form large M–O–C angles to relieve steric strain at the metal. We note that some of the M–O–Si angles in the compound $\mathrm{Mo(OSiMe_3)_4(HNMe_2)_2}$ are greater than 170° which can be attributed to

---

(9) Cotton, F. A.; Walton, R. A. "Multiple Bonds Between Metal Atoms"; Wiley: New York, 1982.

(10) Chisholm, M. H. *Transition Met. Chem.* (*Weinheim, Ger.*) **1978**, *3*, 321.

(11) Chisholm, M. H.; Cotton, F. A.; Murillo, C. A.; Reichert, W. W. *Inorg. Chem.* **1977**, *16*, 1801.

(12) Leonelli, J. Ph.D. Thesis, Indiana University, Bloomington, IN, 1982.

(13) Chisholm, M. H.; Folting, K.; Huffman, J. C.; Rothwell, I. P. *Organometallics* **1982**, *1*, 251.

(14) This argument has been used to explain the large terminal Ti–O–Ph angles in $\mathrm{[TiCl_2(OPh)_2]_2}$. See: Watenpaugh, K.; Caughlan, C. N. *Inorg. Chem.* **1966**, *5*, 1782.

the ability of Si to undergo π bonding to oxygen.[15]

Experimental Section

Preparation of 1,2-$Mo_2(O$-*i*-$Pr)_2(OAr)_4$ (I). To a solution of $Mo_2(O$-*i*-$Pr)_6$ (1.48 g, 2.8 mmol) in benzene (50 mL) was added 2,6-dimethylphenol (HOAr, 2.55 g, 20.9 mmol), and the mixture was allowed to stir for 4 h. Removal of solvent under vacuum, followed by addition of hexane (20 mL), filtration, and cooling to -15 °C gave large red crystals of product.

^1H NMR (30 °C, C_6D_6)^2 δ 6.6-7.0 (m, $OC_6H_3Me_2$), 2.28 (s, $OC_6H_3Me_2$), 5.10 (septet, $OCHMe_2$), 1.11 (d, $OCHMe_2$). A great deal of difficulty was experienced in trying to obtain clean ^1H NMR spectra of this compound. The solution spectra changed slowly over time, showing the buildup of a number of new species. Two of these components were identified from their spectra as 2,6-dimethylphenol and $Mo_2(OAr)_6$ (II) with trace amounts of 2-propanol.

Preparation of $Mo_2(OAr)_6$ (II). By use of the same procedure as above, the solution was stripped and a melt formed between I and the excess phenol at 100 °C for 10 min. Addition of hexane gave the product as an insoluble red powder. Anal. Calcd for $Mo_2C_{48}O_6H_{54}$: C, 62.75; H, 5.92. Found: C, 62.20; H, 6.01. ^1H NMR (30 °C, C_6D_6) δ 6.6-7.1 (m, $OC_6H_3Me_2$), 2.09 (s, $OC_6H_3Me_2$).

X-ray Structural Determination for 1,2-$Mo_2(O$-*i*-$Pr)_2(OAr)_4$ (I). General procedures have been described previously.[16]

A dark red crystal of dimensions 0.25 × 0.30 × 0.30 mm was selected and transferred to the cold stream of the goniostat under an atmosphere of dry nitrogen. The cell dimensions obtained from 36 reflections at -163 °C with Mo Kα (λ = 0.71069 Å) were a = 18.169 (6) Å, b = 11.327 (3) Å, c = 10.678 (3) Å, α = 99.58 (2)°, β = 57.82 (2)°, γ = 97.63 (2)°, Z = 2, d(calcd) = 1.441 g cm^{-3} with space group $P\bar{1}$.

A total number of 4810 reflections were collected by using standard moving-crystal moving-detector techniques with the following values: scan speed = 4.0° min^{-1}; scan width = 2.0 + dispersion; single background time at extremes of scan = 4 s; aperture size = 3.0 × 4.0 mm. The limits of data collection were $6° < 2\theta < 45°$. Of the 4810 reflections, 4731 were unique, and the number with $F > 2.33\sigma(F)$ was 3758.

The structure was solved by direct methods and refined by full-matrix techniques, including all hydrogen atoms, to give final residuals $R(F) = 0.0425$ and $R_w(F) = 0.0406$. The goodness of the fit for the last cycle was 1.223, and the maximum Δ/σ was 0.05.

Acknowledgment. We thank the donors of the Petroleum Research Fund, administered by the American Chemical Society, and the Research Corp. for support of this work.

Registry No. I, 86645-80-9; II, 86667-99-4; $Mo_2(O$-*i*-$Pr)_6$, 62521-20-4; Mo, 7439-98-7.

Supplementary Material Available: Tables of anisotropic thermal parameters and lists of observed and calculated structure factors (38 pages). Ordering information is given on any current masthead page.

---

[15] Chisholm, M. H.; Reichert, W. W.; Thornton, P. *J. Am. Chem. Soc.* **1978**, *100*, 2744.

[16] Huffman, J. C.; Lewis, L. N.; Caulton, K. G. *Inorg. Chem.* **1980**, *19*, 2755.

Contribution from the Centre de Recherches Nucléaires,
67037 Strasbourg Cedex, France

^{161}Dy Mössbauer Spectroscopy Studies of Divalent and Trivalent Dysprosium Halides and Oxyhalides

J. M. FRIEDT,* J. MacCORDICK, and J. P. SANCHEZ

Received February 8, 1983

^{161}Dy hyperfine interaction measurements are reported for the dysprosium dihalides DyX_2, trihalides DyX_3, and oxyhalides DyOX (X = Cl, Br, I) using the 26-keV Mössbauer resonance. In the dihalides, the electron configuration of dysprosium is divalent ($4f^{10}$). However, it has been impossible to obtain pure phases of these compounds. The oxyhalides order antiferromagnetically below 10 K. The hyperfine parameters and the magnetic ordering in these compounds are interpreted in terms of electronic structure with use of a Hamiltonian including electric crystal field and magnetic exchange effects. The change of mean square nuclear radius of ^{161}Dy between the ground and 26-keV levels ($\Delta\langle r^2\rangle = 8.0 \times 10^{-3}$ fm^2) is deduced by combination of the isomer shift results with free-ion electron density calculations.

Introduction

Considerable interest has been devoted recently to the problem of the existence of lanthanide (Ln) ions in valence states other than the common trivalent configuration $4f^n$.[1-5] Whereas the existence and the stability of the divalent Ln^{2+} configuration are well established for the elements of the middle (Sm, Eu) and of the end (Yb) of the lanthanide series, the behavior of some of the other elements is still debated. In halides of composition $LnX_{2\pm x}$, a saltlike character and the occurrence of a valence configuration $4f^{n+1}$ has been demonstrated for the elements Nd, Sm, Eu, Tm, and Yb. On the other hand, for some other elements (e.g. La, Gd), substoichiometric halides $LnX_{2\pm x}$ present a metallic character; this has been concluded from measurements of conductivity, optical absorption, etc.[6] In the latter class of materials, the Ln ion appears to be trivalent, with delocalized electrons responsible for the metallic character.[6] Other substoichiometric halides of the type $LnX_{1\pm x}$ (e.g. LaCl or Er_4I_5) present peculiar structures consisting of metallic clusters with interstitial halide atoms. The Ln ions are probably also trivalent in these systems.[7]

Dysprosium represents a limiting case in this range of behavior since thermodynamic calculations predict that the divalent configuration Dy^{2+} might be at the limit of stability in halide compounds.[8] The existence of a dysprosium chloride, $DyCl_2$, phase and of intermediate chlorides has been established from phase diagram studies.[9] Although conductivity

---

[1] Haschke, J. M. In "Handbook on the Physics and Chemistry of Rare Earths"; Gschneider, K. A., Jr., Eyring, L., Eds.; North-Holland: Amsterdam, 1979; Vol. IV, p 89.

[2] Johnson, D. A. *Adv. Inorg. Chem. Radiochem.* **1977**, *20*, 1.

[3] Bärnighausen, H.; Warkentin, E. *Rev. Chim. Miner.* **1973**, *10*, 141.

[4] Bärnighausen, H. *Proc. Rare Earth Res. Conf., 12th* **1976**, *1*, 404.

[5] Bärnighausen, H. private communication of unpublished results. Bossert, W. Ph.D. Thesis, University of Karlsruhe, 1981. Gütlich, P.; Link, R.; Ensling, J., private communication of unpublished results.

[6] Corbett, J. D. *Rev. Chim. Miner.* **1973**, *10*, 239.

[7] Simon, A. *Angew. Chem., Int. Ed. Engl.* **1980**, *20*, 1.

[8] Kim, Y. C.; Oishi, J. *J. Less-Common Met.* **1979**, *65*, 199.

0020-1669/83/1322-2910$01.50/0